Image Quality Assessment for Fused Remote Sensing Imageries

Mohd Nadzri Md Reba,[a,*] and Ong Juey C'uang[b]

[a]Institute of Geospatial Science and Technology (INSTeG), Universiti Teknologi Malaysia, 81310 UTM Johor Bahru, Malaysia
[b]Department of Geoinformation, Faculty of Geoinformation and Real Estate, Universiti Teknologi Malaysia, 81310 UTM Johor Bahru, Malaysia

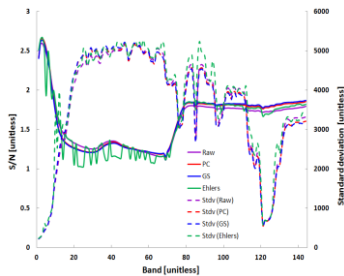[*]Corresponding author: nadzri@utm.my

Graphical abstract

Abstract

Image fusion provides precise information in both spatial and spectral resolutions that benefit significantly in high accuracy mapping. Yet, there is less intention withdrawn in justifying the performance of the fused image. In this study, qualitative and quantitative assessments were carried out to test the quality of fusion image. Principal Component Analysis (PCA), Gram-Schmidt and Ehlers were applied to fuse the hyperspectral and Lidar image. Ehlers fusion showed good in preserving the color of image and contained the most information. Besides, the classification of Ehlers fused image showed the highest accuracy.

Keywords: Image fusion, hyperspectral, image quality

Abstrak

Pelakuran imej memberikan maklumat tepat dari aspek resolusi ruang dan spektral yang dapat membantu dalam pemetaan berketepatan tinggi. Namun begitu, tiada penekanan dalam penilaian hasil pelakuran imej. Dalam kajian ini, penilaian dari segi kualitatif dan kuantitatif dilakukan untuk menilai kualiti imej yang dilakurkan. Teknik *Principal Component Analysis* (PCA), *Gram-Schmidt* dan *Ehlers* digunakan untuk melakurkan imej hyperspektral dan Lidar. Pelakuran melalui teknik *Ehlers* menunjukkan kelebihan dalam mengekalkan warna imej dan mengandungi maklumat yang padat. Disamping itu, pengelasan imej pelakuran dari teknik *Ehlers* memberikan ketepatan yang paling tinggi.

Kata kunci: Pelakuran imej; hyperspectral, kualiti imej

■1.0 INTRODUCTION

Image fusion application on remote sensing is often involved in a process of combining primary image of which is rich in spatial resolution with the secondary image with high spectral resolution to yield fused image which attributes both spectral and spatial information. Fused image in turn provides higher representation and thus significantly enhances interpretation performance of the raw image[1]. Besides, high degree of information acquired by different sensor provides various physical characteristic of ground feature and as a result the accuracy of image interpretation and classification improved[2,3]. Many studies of image fusion have been conducted in last decades though to date, only a few of them had highlighted reliable methods to assess the quality of fused image as reported in the references[4,5,7]. All of these studies were carried out for multispectral image fusion with number of bands is less than 20.In the case of hyperspectral images of which more than 20 bands are used, image fusion conveys rich spectral information in the high resolution pixel. It is a challenge to fuse hyperspectral images where the process demands massive data storage at high cost and time consumption. Study by Kotwal and Chaudhuri[8] had demonstrated quantitative evaluation of hyperspectral image techniques and it has yet limited to accuracy

assessment of fused image classification. This paper presents qualitative and quantitative assessment on image quality of fused image produced from the combination of hyperspectral data and Lidar data. Three fusion techniques were used in this study namely Principal Component Analysis (PCA), Gram Schmidt (GS) and Ehlers fusion techniques. In addition to both quality assessment methods, the accuracy of fused image was validated based on the classification results.

■2.0 DATA AND MATERIALS

2.1 Remote Sensing Data

Set of hyperspectal and Lidar data is acquired from the Data Fusion Technical Committee of the IEEE Geoscience and Remote Sensing Society (GRSS) that provides the data set for the IEEE Image Fusion Competition in 2012. Both imageries show the area within the University of Houston campus and its surrounding urban area. Figure 1 presents image of stadium taken by both systems respectively. The hyperspectral image consists of 144 bands ranging from blue to near infrared wavelength was captured by passive optical sensor during a day. The data was acquired by

the NSF-funded Center for Airborne Laser Mappping (NCALM) and had been calibrated to at-sensor spectral radiance units, hereafter referred as SRU [cm^{2}sr nm]. At the same time, the airborne also carried a Lidar system to collect dense backscattered returns to form massive cloud points on the ground. Each point represents planimetric and elevation attributes. Both images had well registered in local coordinates and projection system. Complete data specification for both acquisition systems is presented in Table 1.
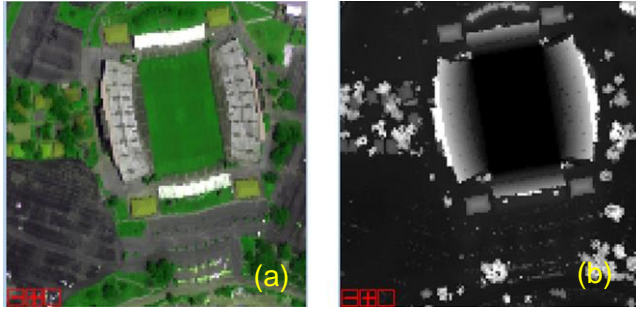
Figure 1 Snapshots of remote sensing data over the stadium. (a) Color composite of hyperspectral image and (b) Intensity Lidar image.

2.2 Ground Spectral Libraries

Spectral feature information for 15 different landcover classes is provided in the form of the region of interest (roi). Each roi data consists of several pixel numbers and the list of each class with its total pixels is represented in Table 2. The roi spectral attribute helps in rendering the image classification and later defining the confusion matrix of classification.

Table 2 Landcover classes provided in roi.

Class	Feature	Pixels	Class	Feature	Pixels
1	Healthy grass	198	9	Road	193
2	Stress grass	190	10	Highway	191
3	Synthetic grass	192	11	Railway	181
4	Tree	188	12	Empty car park lot	192
5	Soil	186	13	Occupied car park	184
6	Water	182	14	Tennis court	181
7	Residents	196	15	Running track	187
8	Commercial	191			

2.3 Data Fusion Techniques

Three unprecedented fusion techniques were applied on the 144-band hyperspectral image for fusing with the Lidar data namely Principal Component Analysis (PCA), Gram-Shchmidt (GS) and Ehlers fusion. Anticipation in the data fusion is to have spectral advantage of hyperspectral and high planimetric accuracy of Lidar spatial resolution together embedded in the fused output.

In principle, the PCA converts inter-correlated hyperspectral bands into new set of uncorrelated components[9] as this fusion technique tends to maintain the original color balance[7]. Besides, PCA is independent to the numbers of bands involved and therefore it is suitable for fusing considerable bands in hyperspectral image[6]. GS technique is a multi-dimensional linear orthogonal transformation which applies approach of linear algebra and multivariate statistics[4]. The procedure is comparable to PCA as both method applied similar statistical variants but the results of GS vary to the input images. Ehlers fusion is a technique used for the spectral preservation in multi-temporal and multi-sensor data[10]. It is based on the Hue-Intensity-Saturation (HIS) transform and the Fast Fourier Transform (FFT)[6,7]. This technique also preserves the best spectral characteristic of original hyperspectral image during the fusion process[10] but the processing is time consuming[6]. The abovementioned fusion techniques are available in many off-the-shelf image processing software.

In this study, all of these fusion techniques are applied to fuse a hyperspectral image of 144 bands at spatial resolution of 2.5 meter with a single band Lidar image with spatial resolution of 2.5 meter. These fusion techniques work in pixel-by-pixel basis[3] so as to improve the spatial resolution and retain the spectral properties of each pixel in the original hyperspectral image[1]. Basically, these techniques keep the numbers of bands so that to provide consistency radiometric information in assessing the image quality of pre- and post-fusion.

■3.0 QUALITATIVE AND QUANTITATIVE IMAGE QUALITY ASSESSMENTS

Image quality assessment was carried out to study the performance of fused image in two aspects of qualitative and quantitative. In the qualitative evaluation, visualization quality was assessed by determining the distinctiveness of pixels in the visual appearance of the scene. Histogram of each fused image was compared with of the raw image and the Gaussian-shape histogram determines the degree of enhancement taken place by each fusion technique. On the other hand, applying statistical variants on each fused image performed the quantitative evaluation. Description of each statistical variant is as follows.

a)   Signal to Noise (S/N)

S/N evaluates the performance of fused image in term of its noise content. By assuming the pixel of fused image behaved in Gaussian form, therefore, the noise is estimated as the standard deviation of fused pixels and the mean represents the estimated "signal" of the fused image as below.

$$\frac{S}{N} = \frac{m}{s} \qquad (1)$$

Table 1 Data specification of Hyperspectral and Lidar

Specification	Platform	Hyperspectral	Lidar
Data & Sensor Specification	Numbers of band	144	1
	Range of wavelength	380 – 1050 nm	1064 nm
	Dimension of image [pixels]	1905 width × 369 height	1905 width × 369 height
	Spatial resolution	2.5 meters	2.5 meters
	Average altitude of sensor	5500 ft	2000 ft
Image Projection	Projection	UTM, Zone 15	UTM, Zone 15
	Spheroid	GRS 1980	GRS 1980
	Datum	NAD 83	NAD 83
Acquisition Time	Date	23 June, 2012	22 June, 2012
	Time	17:37:10 to 17:39:50 UTC	14:27:55 to 15:38:10 UTC
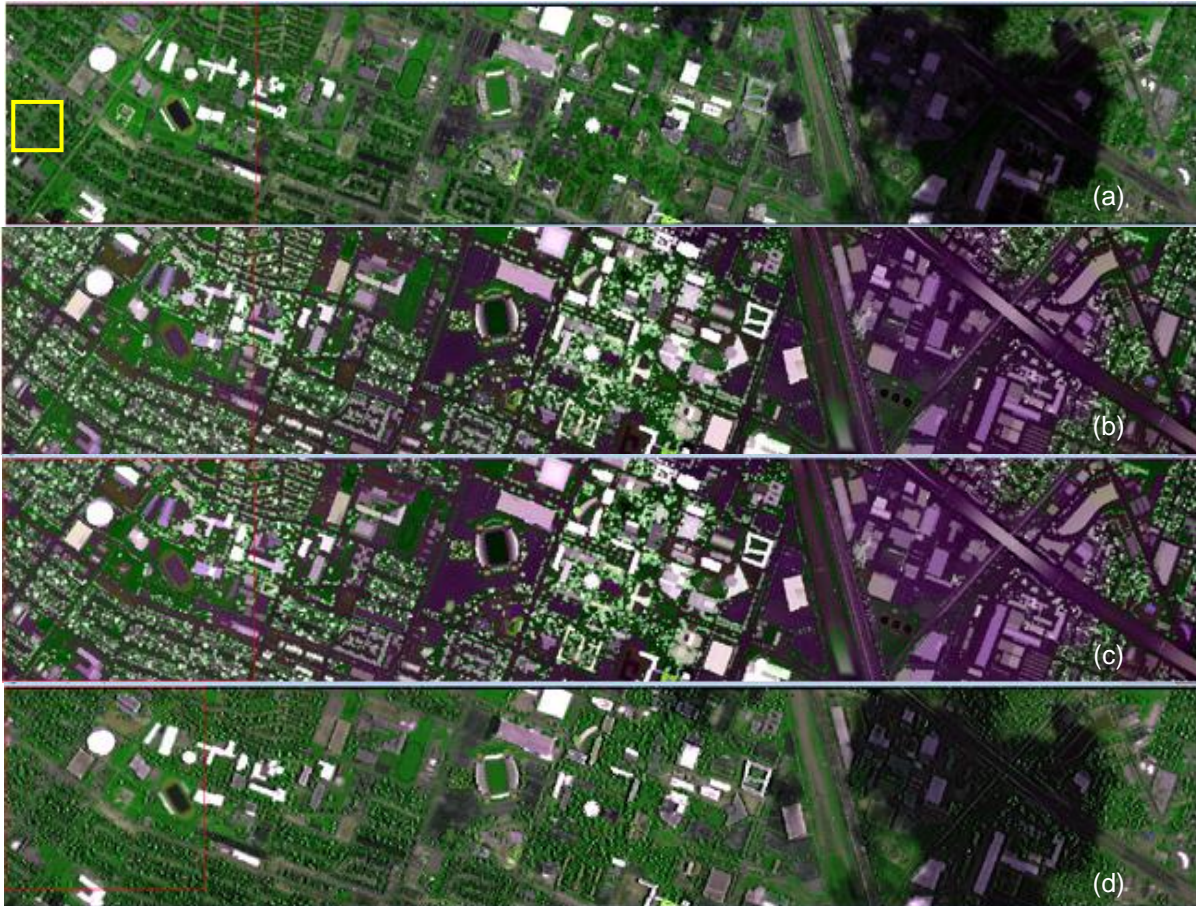
Figure 2 RGB color composition of band 51, 78 and 30 for (a) raw hyperspectral image, (b) PCA fused image, (c) GS fused image and (d) Ehlers fused image. The yellow box outline in (a) is the area of interest used for discussion on the classification result (related to Figure 6).
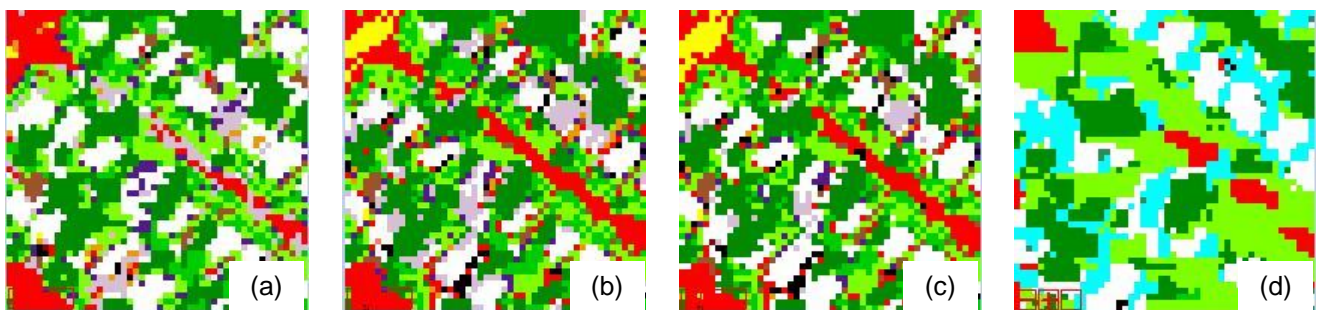
Figure 7 Classified image from different fused images. (a) is the classification results from original hyperspectral image, (b) from PCA fused image, (c) from GS fused image and (d) from Ehlers fused image.

Table 3 Result of quantitative and qualitative analysis of data fusion techniques.

Fusion Techniques	Histogram [cm²sr nm]		Statistics					Classification	
	Mean	Stand. Dev.	Mean [cm²sr nm]	Stand. Dev. [cm²sr nm]	S/N [unitless]	Entropy [%]	Gradient [cm²sr nm]	Overall Acc. [%]	Kappa coeff.
Raw	4266.863	6211.205	5435.275	3625.326	1.589	16.270	126.714	87.32	0.8642
PCA	4148.626	6212.697	5440.130	3610.622	1.605	16.203	117.803	90.11	0.8941
GS	4181.192	6212.861	5446.544	3610.794	1.609	16.347	124.581	89.44	0.8869
Ehlers	4389.637	6409.783	5613.820	3793.768	1.569	18.110	318.172	94.81	0.9443

where μ is the mean and σ is the standard deviation calculated from the image of each band as in Eq.(2) and (3) respectively as the followings.

$$\mu = \frac{1}{M \times N} \sum_{i=1}^{M} \sum_{i=1}^{N} G(X_{i,j}) \qquad (2)$$

$$\sigma = \sqrt{\sum_{i=1}^{M} \sum_{i=1}^{N} \left(G(X_{i,j}) - \mu \right)^2 / (M \times N)} \qquad (3)$$

where *M* and *N* are the numbers of row and column of image, $G(X_{i,j})$ is the grey value of each pixel in *i* and *j* pixel index.

b)   Entropy

Entropy indicates the amount of the information content in the fused image. Higher entropy indicates the image is rich with information content. Entropy, *H* can be defined as follows.

$$H = -\sum_{i=1} P_i \log P_i \qquad (3)$$

where $P(x_i)$ represent the histogram of the image.

c)   Average of gradient

The average of gradient, *g,* is the measure of image sharpness in terms of gradient values and represents the ability of an image to present fine details contrast. The formulation is presented as follows.

$$\bar{g} = \frac{1}{M \times N} \sum_{i=1}^{M} \sum_{i=1}^{N} \sqrt{\frac{(\frac{\delta I(x_i, y_i)}{\delta x_i})^2 + (\frac{\delta I(x_i, y_i)}{\delta y_i})^2}{2}} \qquad (4)$$

where $I(x_i, y_i)$ is the grey value of each pixel.

Supervised classifications namely Parellelpiped, Minimum Distance, Spectral Angle Mapper (SAM), Neural Network (NN), Mahalonobis Distance and Support Vector Machine (SVM) are applied on the fused images by incorporating all 15 spectral classes of landcover that are used to train and finally to compute the classification accuracy. To assess the accuracy retrieved the confusion matrix is used in which the overall accuracy and the kappa coefficient are simultaneously estimated.

■4.0 RESULTS AND ANALYSIS

4.1 Qualitative Analysis

Figure 2 shows the RGB color composite of raw hyperspectral image (2a) and three fused images (2b to 2d) with band 51, 78 and 30 bands combination. PCA (2b) and GS (2c) give higher contrast among the objects with the background especially at the edge of the object. PCA conveys sharper color and higher contrast pixels than in GS fused image of which pixels is slightly darker and blurred. Ehlers demonstrates the best color preservation, as most of the features remained the same as in the raw image but with higher texture from the Lidar. As a result, the edges of the object are significantly more obvious and easier to identify. Figure 3 presents the histogram of pixels at band 74 and pixel density distribution of Ehlers is fairly expended in shape that is basically provide more pixel information and higher contrast to background.
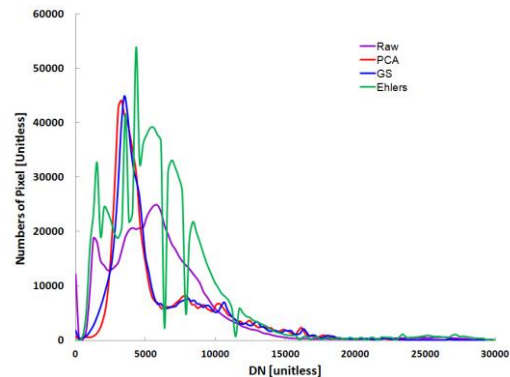
**Figure 3** Histogram of pixels in raw and fused images at band 74.

4.2 Quantitative Analysis

Figure 4 shows result of S/N presented in the primary ordinate with the standard deviation in the secondary ordinate for all fusion techniques performed in each band.
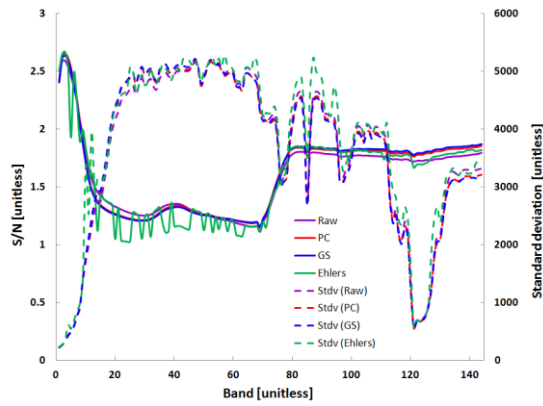
Figure 4 Plot of S/N and the standard deviation of raw and fused images for each band.

The estimated noise (i.e., the standard deviation) with low values increases the S/N. The S/N of Ehlers is inconsistent from band to band due to the variation from its fine contrast pixel and is lower particularly for band 1 to 76 as in this band range the Ehlers image has higher contrast than other fused images.
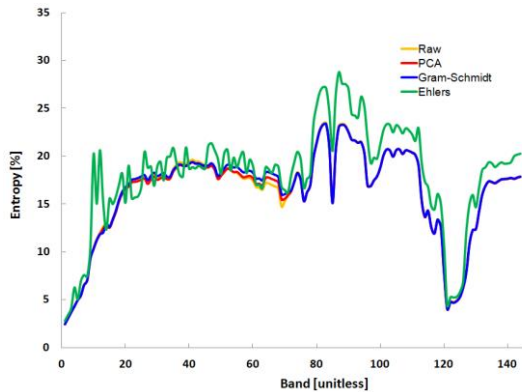
Figure 5 Plot of entropy of raw and fused images for each band.

In Figure 5, Ehlers gives higher entropy estimate for each band and this in favor to color richness contained by preserving spectral and spatial information from both raw images as clearly visualized in Figure 2(d). This is also evident in Figure 6 as the fused image of Ehlers has significant gradient estimate and this indicates that the visualization quality, which is related to the texture, is outstanding. Average gradient measures the spatial quality where higher average gradient represents higher spatial resolution[11]. It is therefore proved that Ehler fused image has high contrast objects with clearly and easily seen edges.
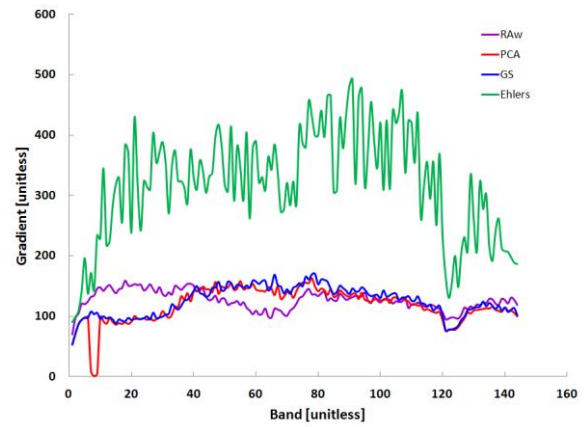
Figure 6 Plot of gradient of raw and fused images for each band.

4.3 Image classification accuracy assessment

Figure 7 shows classified image of different fusion technique respectively. To validate the fusion results, confusion matrix was computed for each classification image and overall accuracy is determined in Table 3. Based on the classification results, Ehlers shows homogeneous classified features in solid polygons that indicated small numbers of mixed pixel with a classified feature. However, misclassification is evident particularly for the group of pixels representing very small object on the ground. This is not a case for PCA and GS as landcover is better classified but contaminated by mixed pixels (where some black pixels are evident). In term of classification accuracy, Ehlers achieved the highest accuracy of 94.8% and this has proven the Ehlers technique implies the highest quality of fused image (completely summarized in Table 3) qualitatively and quantitatively. By comparing the Ehlers's fused image with the original image, the classification results had improved significantly as the features of different classes more clear to be identified.

■5.0 CONCLUSION

This study addressed image quality improvement from the image fusion. The fusion image shows better visualization quality than the raw image. This study found that Ehlers fusion technique produced the best result of qualitative, quantitative and classification assessments. Ehlers preserves well the color and contrast of the image. The analysis showed that Ehlers is rich with spatial and spectral information.

References

[1]   J. Zhang. 2010. *Int. J. Image and Data Fusion*. 1 : 5–24.
[2]   C. Pohl, J.L.Van Genderen. 1998. *Int. J. Remote Sensing*. 19 : 823–854.
[3]   D. Jiang, D. Zhuang, et al. 2011. *Image Fusion and Its Applications*. 1.
[4]   H. Liu and X. Zhang. 2009. *Urban Remote Sensing Event*. 1–6.
[5]   D. Chao, H. Li, J. Han. 2011. *Advances in Computer Science, Intelligent System and Environment*, Springer. 104 : 169–173.
[6]   S. Klonus, M. Ehlers. 2009. *Int. Conf. on Information Fusion*. 1409–1416.
[7]   A.K. Helmy, A.H. Nasr, et al. 2010. *Int. J. Computer*. 4 : 107–115.
[8]   K.Kotwal, S. Chaudhuri. 2013. *Information Fusion*. 14 : 5–18.
[9]   D. Jiang, D. Zhuang, et al. 2009. *Sensors*. 9 : 7771–7784.
[10]   D. Amarsaikhan, H.H. Blotevogel, et al. 2010. *Int. J. Image and Data Fusion*. 1 : 83–97.
[11]   M. Fallah Yakhdani, A. Azizi. 2010. *ISPRS Conf. Vienna*. XXXVIII : 204–209.